

University of Nebraska - Lincoln

DigitalCommons@University of Nebraska - Lincoln

---

Papers in Natural Resources

Natural Resources, School of

---

8-31-2022

## Using Electrochemical Oxidation to Remove PFAS in Simulated Investigation-DerivedWaste (IDW): Laboratory and Pilot-Scale Experiments

Amy Yanagida

Elise Webb

Clifford E. Harris

Mark Christenson

Steven Comfort

Follow this and additional works at: <https://digitalcommons.unl.edu/natrespapers>



Part of the [Natural Resources and Conservation Commons](#), [Natural Resources Management and Policy Commons](#), and the [Other Environmental Sciences Commons](#)

---

This Article is brought to you for free and open access by the Natural Resources, School of at DigitalCommons@University of Nebraska - Lincoln. It has been accepted for inclusion in Papers in Natural Resources by an authorized administrator of DigitalCommons@University of Nebraska - Lincoln.

## Article

# Using Electrochemical Oxidation to Remove PFAS in Simulated Investigation-Derived Waste (IDW): Laboratory and Pilot-Scale Experiments

Amy Yanagida <sup>1</sup>, Elise Webb <sup>2</sup>, Clifford E. Harris <sup>3</sup>, Mark Christenson <sup>2</sup> and Steve Comfort <sup>1,\*</sup> <sup>1</sup> School of Natural Resources, University of Nebraska, Lincoln, NE 68583, USA<sup>2</sup> AirLift Environmental, LLC, 5900 N. 58th, Suite 5, Lincoln, NE 68583, USA<sup>3</sup> Department of Chemistry, Albion College, Albion, MI 49224, USA

\* Correspondence: scomfort@unl.edu; Tel.: +1-402-472-1502

**Abstract:** Repeated use of aqueous firefighting foams at military aircraft training centers has contaminated groundwater with per and polyfluorinated alkyl substances (PFAS). To delineate the extent of PFAS contamination, numerous site investigations have occurred, which have generated large quantities of investigation-derived wastes (IDW). The commonly used treatment of incinerating PFAS-tainted IDW is costly, and was recently suspended by the Department of Defense. Given long-term IDW storage in warehouses is not sustainable, our objective was to use electrochemical oxidation to degrade PFAS in contaminated water and then scale the technology toward IDW treatment. This was accomplished by conducting a series of laboratory and pilot-scale experiments that electrochemically oxidized PFAS using direct current with boron-doped diamond (BDD) electrodes. To improve destruction efficiency, and understand factors influencing degradation rates, we quantified the treatment effects of current density, pH, electrolyte and PFAS chain length. By using <sup>14</sup>C-labeled perfluorooctanoic acid (PFOA) and tracking temporal changes in both <sup>14</sup>C-activity and fluoride concentrations, we showed that oxidation of the carboxylic head (<sup>-14</sup>COOH → <sup>14</sup>CO<sub>2</sub>) was possible and up to 60% of the bonded fluorine was released into solution. We also reported the efficacy of a low-cost, 3D printed, four-electrode BDD reactor that was used to treat 189 L of PFOA and PFOS-contaminated water (C<sub>0</sub> ≤ 10 µg L<sup>-1</sup>). Temporal monitoring of PFAS with LC/MS/MS in this pilot study showed that PFOS concentrations decreased from 9.62 µg L<sup>-1</sup> to non-detectable (<0.05 µg L<sup>-1</sup>) while PFOA dropped from a concentration of 8.16 to 0.114 µg L<sup>-1</sup>. Efforts to improve reaction kinetics are ongoing, but current laboratory and pilot-scale results support electrochemical oxidation with BDD electrodes as a potential treatment for PFAS-tainted IDW.

**Keywords:** boron-doped diamond electrodes; per and polyfluorinated alkyl substances; chemical oxidation; <sup>14</sup>C-labeled PFOA



**Citation:** Yanagida, A.; Webb, E.; Harris, C.E.; Christenson, M.; Comfort, S. Using Electrochemical Oxidation to Remove PFAS in Simulated Investigation-Derived Waste (IDW): Laboratory and Pilot-Scale Experiments. *Water* **2022**, *14*, 2708. <https://doi.org/10.3390/w14172708>

Academic Editors: Yujue Wang, Dionysios (Dion) Demetriou, Dionysiou and Huijiao Wang

Received: 22 July 2022

Accepted: 20 August 2022

Published: 31 August 2022

**Publisher's Note:** MDPI stays neutral with regard to jurisdictional claims in published maps and institutional affiliations.



**Copyright:** © 2022 by the authors. Licensee MDPI, Basel, Switzerland. This article is an open access article distributed under the terms and conditions of the Creative Commons Attribution (CC BY) license (<https://creativecommons.org/licenses/by/4.0/>).

## 1. Introduction

Per- and polyfluoroalkyl substances (PFAS) are a family of synthesized chemicals that have been heavily used in manufacturing, often without adequate disposal. Commonly used to improve the quality of commercial products by making them resistant to heat, oil, and stains, PFAS are found in many household goods and industrial products such as surfactants, emulsifiers, and aqueous film forming foams (AFFFs). Due to their unique ability to resist heat and block oxygen, PFAS-containing firefighting foams were used at aircraft service centers where fire-fighting training operations were routinely performed. With more than three decades of repeated use at hundreds of military facilities across the U.S.A., PFAS have been detected in 61% of the groundwater samples taken around Department of Defense (DoD) facilities with concentrations ranging from µg L<sup>-1</sup> (ppb) to low mg L<sup>-1</sup> (ppm) concentrations [1–4].

Chemically, PFAS contain both a fluorinated carbon tail and a hydrophilic ionic head ( $-\text{COOH}$ ,  $-\text{SO}_3\text{H}$ ), and it is this unique structure that give PFAS their biphasic or surfactant characteristics. The PFAS molecule may be either fully (per-) or partially (poly-) fluorinated and can contain between two and eighteen carbon atoms [5]. Examples of the most common PFAS include perfluorooctanoic acid (PFOA;  $\text{C}_8\text{F}_{15}\text{O}_2\text{H}$ ) and perfluorooctane sulfonic acid (PFOS;  $\text{C}_8\text{F}_{17}\text{SO}_3\text{H}$ ). Although PFOA and PFOS are the two most frequently detected PFAS in contaminated aquifers, there are literally hundreds of PFAS precursors that have been released into the environment, which are also causes for concern.

Unfortunately, the chemical properties that make PFAS useful from an industrial perspective also make them mobile and recalcitrant once released into the environment. As true xenobiotics, PFAS have no known natural decomposition processes and the stability of the C-F bond makes them almost un-degradable by natural attenuation [6,7].

Now that toxicological studies have revealed the bio-accumulative, neurotoxic, and potentially carcinogenic nature of PFAS exposure [8–11], identifying and delineating the extent of PFAS contamination is paramount for protecting human and ecological health. Given the United States Environmental Protection Agency (USEPA) recently decreased its 2016 health advisor level (HAL) of  $70 \text{ ng L}^{-1}$  (70 parts per trillion, 70 ppt) for the singular or combined concentration of PFOA and PFOS, to  $0.004 \text{ ng L}^{-1}$  for PFOA and  $0.02 \text{ ng L}^{-1}$  for PFOS [12], the need to further delineate the extent of PFAS contamination in aquifers will only intensify.

The federal government has an environmental responsibility to delineate the extent of contamination at sites where firefighting foams were routinely used. While PFAS-contaminated groundwater is the primary concern, site investigations create a secondary problem that is continuing to grow, namely, the generation of investigation-derived waste (IDW). IDW is the water, soil and drill cuttings generated during well installations and sampling activities performed during contaminated site investigations. The potential risks and liabilities associated with PFAS exposure has previously caused IDW generators to take the conservative approach of incinerating their PFAS waste. While energy intensive and costly, incineration offered a workable solution. The temporary moratorium on incinerating PFAS-containing substances by the Department of Defense [13] has now changed the way IDW will be handled, and complicates disposal options. Given that PFAS site investigations will continue and long-term storage of containerized IDW in warehouses is not a sustainable solution, alternative treatment options are needed. In 2020, the EPA established the PFAS Innovative Treatment Team (PITT) to address the disposal and destruction of PFAS-containing media and waste. This PITT team identified four technologies with the potential to destroy PFAS-contaminated media and waste [14]; one of these technologies was electrochemical oxidation (EC).

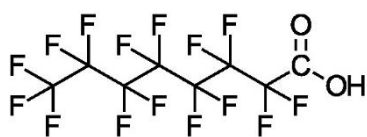
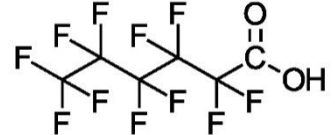
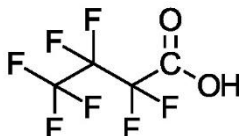
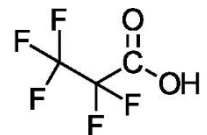
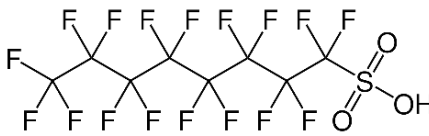
As an alternative to incinerating PFAS-tainted IDW, we report herein on a series of laboratory and pilot-scale experiments that electrochemically oxidized PFAS with boron-doped diamond electrodes (EC-BDD) with direct current. The reason BDD anodes can degrade per- and polyfluoroalkyl substances is because of the greater overpotential they require to oxidize water to oxygen (relative to other anodes). The oxygen overpotential for gold, platinum, or glassy carbon anodes ranges between 1.7 and 2.2 V, but up to 2.5 V for BDD anodes [15]. This allows BDD electrodes to produce direct anodic oxidation of the PFAS and offer a “chemical-free” treatment for PFAS-contaminated water [16]. Our objectives were to quantify the effects of current density, pH, electrolyte and PFAS chain length on degradation kinetics and defluorination. We also report on the efficacy of a custom designed, 3D printed, electrode chamber where the number of BDD electrodes (2 vs. 4), power sources (1 vs. 2) and DC polarity switching, were varied. We then show the results from treating a 208 L (55 gal) container of PFOA- and PFOA-tainted water ( $C_0 = <10 \text{ } \mu\text{g L}^{-1}$ ).

## 2. Materials and Methods

### 2.1. Chemicals

Chemicals were purchased from a variety of vendors and used as received. These chemicals included: perfluorooctanoic acid (PFOA;  $C_8F_{15}O_2H$ ; >95% purity) and perfluorooctane sulfonate (PFOS;  $C_8F_{17}SO_3$ ; >95% purity) (Fisher, Fair Lawn, NJ, USA). Shorter chain PFAS included: perfluorohexanoic acid, perfluorobutyric acid; perfluorohexanesulfonic acid, and perfluorobutanesulfonic acid (Fisher, Fair Lawn, NJ; >98% purity) (Table 1). We also used  $^{14}C$ -labeled perfluorooctanoic acid ( $^{14}C$ -PFOA; 55 mCi mmol $^{-1}$ ; American Radiolabeled Chemicals, St. Louis, MO, USA); sodium sulfate, ammonium fluoride, and  $H_2SO_4$  (Fisher, Fair Lawn, NJ, U.S.A.). All solutions were prepared with Millipore water (18.2 M $\Omega$  cm $^{-1}$  resistivity, 25 °C) from a Nanopure Barnstead E-pure system (Thermo Scientific, Waltham, MA, USA).

**Table 1.** Compound name, acronym, formula, and structure of PFAS used in laboratory and pilot-scale experiments.

Compound (C#)	Acronym	Formula	Structure
Perfluorooctanoic Acid (C8)	PFOA	$F(CF_2)_7COOH$	
Perfluorohexanoic Acid (C6)	PFHxA	$F(CF_2)_5COOH$	
Perfluorobutyric Acid (C4)	PFBA	$F(CF_2)_3COOH$	
Perfluoropropionic Acid (C3)	PFPrA	$F(CF_2)_2COOH$	
Perfluorooctane Sulfonic Acid (C8)	PFOS	$F(CF_2)_8SO_3H$	

### 2.2. Chemical Analysis

Carbon-14 activity ( $^{14}C$ -activity) was determined by removing 1 mL subsamples from the batch reactors and mixing with 6 mL of Ultima Gold liquid scintillation cocktail (Packard, Meriden, CT, USA). Samples were then mixed and allowed to sit overnight in the dark before analyzing on a Packard 1900TR liquid scintillation counter (LSC; Packard Instrument, Downers Grove, IL, USA). A blank consisting of 6 mL Ultima Gold liquid scintillation cocktail was analyzed prior to running the samples and used to correct sample activity values (dpm).

Treating PFAS by electrochemical oxidation removes fluoride from the alkyl chain. Thus, temporal release of fluoride into solution can be representative of PFAS degradation. In select electrochemical experiments, samples were taken during treatment for fluoride analysis and run on a Dionex DX-120 ion chromatograph (IC). Standard solutions of fluoride were first prepared and injected into the IC to create a calibration curve.

Standards were made using ammonium fluoride. The fluoride standards used varied between 1 and 75 mg L<sup>-1</sup>, depending on the concentration of PFAS treated. Choosing which standards to use for data analysis was based on the potential mass of fluoride that could be released into solution by breaking the C-F bonds. For example, defluorination of 10 mg L<sup>-1</sup> PFOA could produce approximately 6.8 mg L<sup>-1</sup> of fluoride; 100 mg L<sup>-1</sup> PFOA could yield 68 mg L<sup>-1</sup> fluoride, if defluorination was complete. All fluoride standards were run through the IC, and peak areas were used to generate a calibration curve through linear regression.

When <sup>14</sup>C-PFOA was not used in experiments, unlabeled PFOA and PFOS concentrations were determined at the University of Nebraska Water Center using a Waters Xevo TQ-S Micro triple quadrupole mass spectrometer with a 2D ultrahigh pressure liquid chromatography interface. Using EPA Method 533 [17], linear calibration curves were obtained for the concentration range of 0–20 µg L<sup>-1</sup> using isotopically labelled internal standards. Specific standard concentrations included: 0, 0.1, 0.5, 1.0, 5, 10 and 20 µg L<sup>-1</sup>. Limit of detection (LOD) and limit of quantification (LOQ) for the analytical method were determined by the following: duplicate analyses of standards; results from samples fortified at a concentration near the low calibration standard signal sensitivity; and the Student's *t*-test value for the number of replicates analyzed.

### 2.3. Electrochemical Experiments

#### 2.3.1. Generalized Setup of Electrochemical Experiments

Most electrochemical experiments were run under similar stirred, single batch conditions. The typical experimental setup consisted of a 600 mL Erlenmeyer flask filled with 500 mL of a PFAS solution (8 µg L<sup>-1</sup> to 100 mg L<sup>-1</sup>). Enough electrolyte salt (Na<sub>2</sub>SO<sub>4</sub>) was added to bring the concentration to 10 mM Na<sub>2</sub>SO<sub>4</sub>. The solution was then spiked with 1 to 3 mL of stock <sup>14</sup>C-PFOA (55 mCi mmol<sup>-1</sup>), which brought the solution's <sup>14</sup>C-activity to approximately 1500 to 3000 dpms mL<sup>-1</sup> and 0.6 mL of diluted H<sub>2</sub>SO<sub>4</sub> acid (10% *v/v* with H<sub>2</sub>O) to decrease the solution pH (2.5). The experimental unit received a magnetic stir bar, was placed on a stir plate, and then mixed at a stir speed of 700 rpm. We used either one boron-doped diamond (BDD) anode and a platinum coated titanium (Pt/Ti) wire cathode, or two boron-doped diamond electrodes (NeoCoat<sup>®</sup>, La Chaux-de Fonds, Switzerland). The NeoCoat<sup>®</sup> electrodes consisted of a polycrystalline boron-doped diamond coating (5 µm coating, 2500 ppm B) deposited on both sides of a mesh niobium substrate. The dimensions of the mesh BDD electrodes were 25 × 100 × 1.4 mm. A plastic holder was fabricated that maintained an electrode spacing of 5 mm. These electrodes were connected to a DC power supply (30 V/20 A, Exttech instruments, Nashua, NH, USA) and suspended in the solution so that they were submerged as fully as possible without the electrical alligator clips touching the solution. Electrical current was set at either 1 or 0.4 A, unless specified otherwise in presented graphs. Assuming an estimated electrode surface area of 25 cm<sup>2</sup>, current densities ranged from 8 to 40 mA cm<sup>-2</sup>. The supplied voltage varied with current density and electrolyte concentration and is reported on resulting graphs.

#### 2.3.2. Effect of Electrical Current

Using a BDD anode and cathode, we quantified the effects of electrical current on a 100 mg L<sup>-1</sup> perfluorooctanoic acid (0.24 mM PFOA) solution. Three separate experiments were run with the electrical current set at 0.2, 0.4 and 1 A (8, 16, 40 mA cm<sup>-2</sup>). The experiments ran for 6 h, and 1.5 mL samples were periodically removed from the stirred reactor to quantify temporal decreases in <sup>14</sup>C-activity. One milliliter samples were mixed with LSC cocktail and analyzed in a liquid scintillation counter; <sup>14</sup>C concentrations were then fit to a first-order rate expression ( $C = C_0 e^{-kt}$ ) and compared.

Preliminary experiments were also run with low concentrations of PFOS (17 µg L<sup>-1</sup>) and PFOA (4.4 µg L<sup>-1</sup>), utilizing the BDD anode and cathodes and 8 mA cm<sup>-2</sup>. These experiments were analyzed with a Micromass Quattro Micro Triple quadrupole liq-

uid chromatograph/mass spectrometer with methods and results presented in the Supplementary Materials (SM).

### 2.3.3. Effect of Acid Addition (pH)

The effect of pH on PFOA degradation was determined by conducting parallel experiments using either two BDD electrodes, or a BDD/Pf/Ti electrode set, both run at an electrical current of 1 A ( $40 \text{ mA cm}^{-2}$ ). The PFAS test solution was a  $100 \text{ mg L}^{-1}$  perfluorooctanoic acid ( $0.24 \text{ mM}$  PFOA) solution, spiked with  $^{14}\text{C}$ -PFOA. We acidified the PFOA solution with diluted  $\text{H}_2\text{SO}_4$  to a pH of 2.5 and left one companion solution untreated (no acid, pH 6–7). Batch reactors were run under the same conditions as above with volts ranging from 16 to 20 V.

### 2.3.4. Effect of Electrolyte

Using the generalized electrochemical procedures and two BDD electrodes as anode and cathode, degradation of PFOA was compared in a  $10 \text{ mM Na}_2\text{SO}_4$  electrolyte salt versus a  $100 \text{ mM KH}_2\text{PO}_4$  salt concentration. The pH of both solutions was adjusted to 2.5 before starting electrochemical oxidation.

### 2.3.5. The Effects of Reseeding PFOA and Fluoride on Degradation

Following the generalized procedures,  $^{14}\text{C}$ -PFOA was reseeded into the stirred batch reactor and treated with two BDD electrodes at pH 2.5. Reseeding occurred at 2 h and 4 h after the initial ( $T = 0 \text{ h}$ ) experiment was started. Temporal samples were taken every 15 min, mixed with the cocktail, and analyzed by LSC.

To determine how fluoride released into solution was possibly influencing BDD performance, we conducted an experiment where generalized procedures were used to treat a  $40 \text{ mg L}^{-1}$  fluoride solution for 2 h before spiking with  $^{14}\text{C}$ -PFOA and tracking changes in  $^{14}\text{C}$  activity. A similar experiment was performed where  $40 \text{ mg F}^{-1} \text{ L}^{-1}$  was treated for 2 h and then spiked with a higher PFOA concentration ( $100 \text{ mg L}^{-1}$  PFOA) so that defluorination could also be monitored.

### 2.3.6. Measuring Defluorination

To measure electrochemical oxidation and defluorination together, we used a  $100 \text{ mg L}^{-1}$  PFOA solution and spiked it with  $^{14}\text{C}$ -PFOA. Using two BDD electrodes and direct current, we removed solution samples from the batch reactor every 30 to 60 min for 6 h.  $^{14}\text{C}$  activity was determined by mixing 1 mL of sample with 6 mL of cocktail and counting on an LSC. Fluoride was measured directly with a Dionex DX-120 ion chromatograph using conductivity detection.

To determine how initial concentration influenced defluorination, we treated PFOA concentrations of 5, 10, 50 and  $100 \text{ mg L}^{-1}$  and ran them under standard EC conditions using an electrical current of 0.4 A ( $8 \text{ mA cm}^{-2}$ ; 12–14 V). Similarly, we determined how fluorinated alkyl chain length influenced the rate of defluorination. We used perfluorinated carbonates with carbon chains lengths of 8, 6, 4, and 3 carbons; specifically, these compounds included perfluorooctanoic acid (C8), perfluorohexanoic acid (C6), perfluorobutyric acid (C4), and perfluoropropionic acid (C3) (Table 1). The starting concentration of each compound was  $0.24 \text{ mM}$ , and each compound was treated with two BDD electrodes and run under standard conditions and 0.4 A.

### 2.3.7. Pilot-Scale Experiments

A 208 L barrel was filled with 189 L of tap water and spiked to  $\sim 10 \text{ } \mu\text{g L}^{-1}$  PFOA,  $\sim 10 \text{ } \mu\text{g L}^{-1}$  PFOS with a  $10 \text{ mM Na}_2\text{SO}_4$  background matrix. We used a custom 3D printed four-electrode, flow-through reactor that allowed the electrodes to fit perfectly into a 3D mold and force contact with the PFAS molecules. The custom reactor was designed with the 3D CAD software SOILDWORKS (Dassault Systèmes Solidworks, Co., Waltham, MA, USA) and then printed on MakerBot Replicator 3D printer (Brooklyn, NY, USA) using MakerBot

filament plastic. To further seal the reactor, flex sealant was used around the periphery of the angular joints and hose connections while a silicone adhesive sealant was used around each electrode. Reactor pieces and electrodes were assembled with 6 mm foam gaskets inserted between each section; electrodes were spaced 1 cm apart. PVC hose adaptors for inlet and outlets were connected to 3D printed material using PVC primer and glue. The final reactor design was fabricated to be semi-permanent (i.e., leak free), but still allowed for disassembly and electrode replacement.

Once constructed, the BDD reactor was connected to a custom designed direct current system (3E, Windsor Heights, IA, USA) that had a 500 W rheostat capable of adjusting current (0–16 A), 4 solid state relays for switching polarities, and two timers for adjusting positive and negative cycles. Pilot-scale experiments were run at 1 A with polarity reversed every 30 s. Tubing adaptors and a submersible pump were used to continuously circulate water through the reactor at a rate of 2.33 L min<sup>-1</sup>. This flow rate allowed the 189 L of simulated IDW to cycle through the BDD reactor every 81 min. Temporal 1.5 mL samples were collected over 450 h and analyzed via LC/MS/MS.

Before treating the pilot-scale 208 L drum of PFAS-contaminated water, the assembled reactor was used to treat multiple batches of 2 L of 10 µg L<sup>-1</sup> of PFOA in a 10 mM Na<sub>2</sub>SO<sub>4</sub> matrix at a flow rate of 1.7 L min<sup>-1</sup>. Variables tested with the 3D printed reactor were the number of BDD electrodes (2 vs. 4), power sources (1 vs. 2) and polarity (constant vs. switching).

### 3. Results and Discussion

#### 3.1. Electrochemical Oxidation of PFAS

A series of laboratory batch experiments were undertaken using a boron-doped diamond (BDD) anode to electrochemically (EC) oxidize PFAS compounds. The advantage electrochemical oxidation has over other technologies, is that BDD anodes can initiate an electron removal from both the ionic heads of PFOA and PFOS-like structures [18–22] (Figure 1). The key factor for enhanced oxidation via EC-BDD treatment is the interaction the EC-generated hydroxyl radicals have with the electrode surface. In general, high oxidation power anodes are characterized by weak electrode–hydroxyl radical interactions resulting in a high current efficiency for organic oxidation and a low electrochemical activity for oxygen evolution. Based on this, boron-doped diamond can be considered as one of the ideal anode materials for electrochemical mineralization of organic contaminants [23].

While the exact mechanisms for electrochemical oxidation of PFAS are complex and still being investigated, there is general agreement that the rate-limiting step is the direct electron transfer at the anode, which results in cleavage of the head group (–COOH vs. –SO<sub>3</sub>H) to produce the corresponding perfluoroalkyl radical (Figure 1); the perfluoroalkyl radical can then quickly react with •OH, O<sub>2</sub>, or H<sub>2</sub>O and degrade to the one-carbon shorter perfluoroheptanecarboxylate (i.e., perfluoro alkyl carbonate, Figure 1). The newly produced, 1-carbon shorter carboxylate then undergoes the same degradation cycle as the original PFOA, sequentially converting the carboxylic acid head to carbon dioxide, the fluorine atoms to hydrogen fluoride, and the CF<sub>2</sub> to another carboxylic acid group.

As discussed by Radjenovic et al. [16], the use of high PFAS concentrations (i.e., 10–100 mg/L) in laboratory experiments likely overestimates EC oxidation performance and makes extrapolating results to environmentally relevant matrices difficult. While we used high PFOA concentrations when fluoride analysis was also performed, the use of <sup>14</sup>C-PFOA provided the advantage of making analysis simple, quick, and negated any PFAS cross contamination interferences. Moreover, by measuring the <sup>14</sup>C activity of the solution (dpms mL<sup>-1</sup>), converting to µCi, and then using the specific activity of the PFOA label (55,000 µCi mmol<sup>-1</sup>), the PFOA concentration could be calculated. In most batch experiments that used only <sup>14</sup>C-PFOA, the typical starting concentrations (C<sub>0</sub>) were 6.8 to 10 µg PFOA L<sup>-1</sup>, which would be environmentally relevant for many contaminated IDW matrices.

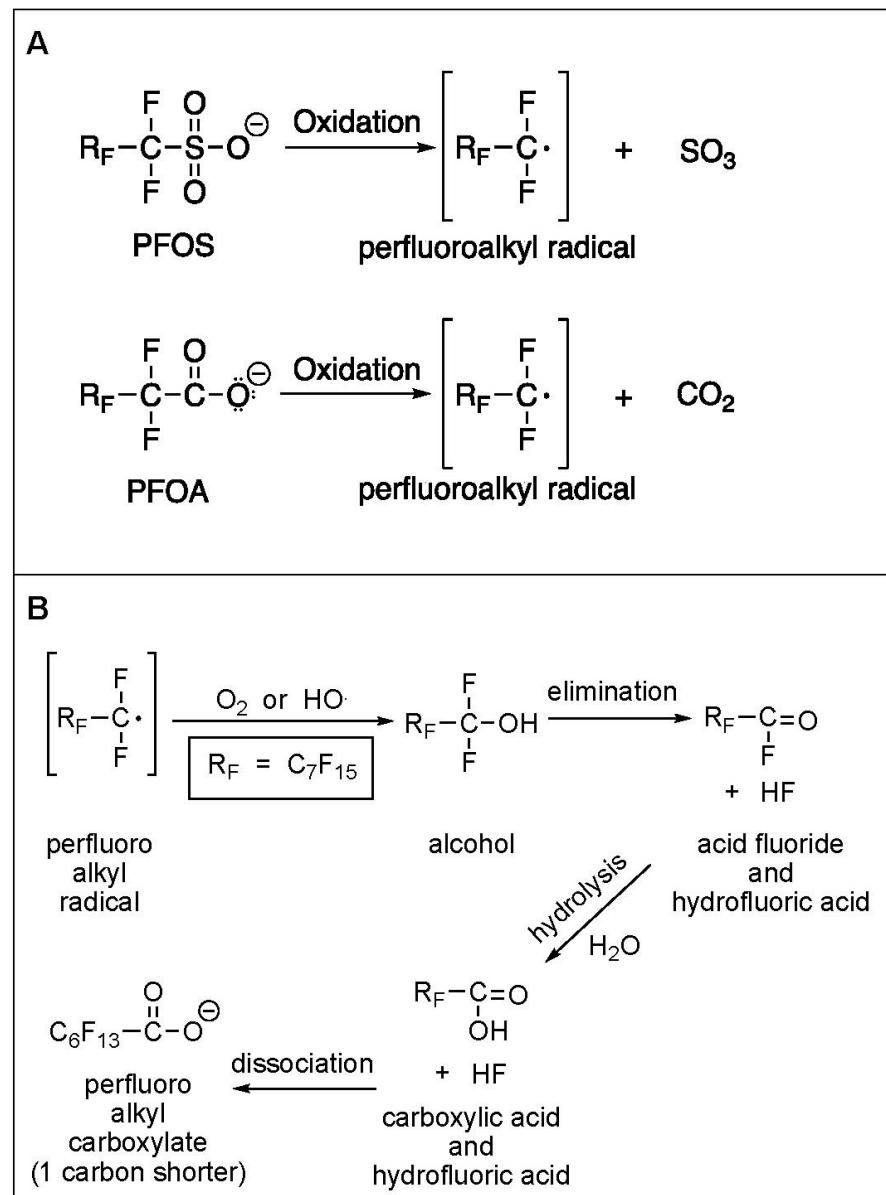


**Figure 1.** (A) Rate-limiting step for the treatment of PFOS versus PFOA to the perfluoroalkyl radical; (B) subsequent degradation of perfluoroalkyl radical.

### 3.2. Effect of Electrical Current

Potential is the major driving force for electrochemical oxidation of PFAS. Applied current density is a key experimental parameter that affects PFAS degradation and defluorination efficiency because it regulates the capability of the electron transfer rate and OH radical generation on the electrode surface. In the PFOA decomposition process, Ochiai et al. [24] found that when the current density was higher than 0.6 mA/cm<sup>2</sup>, the direct electron oxidation was no longer the main mechanism. Using DC settings that would produce 0.6 mA/cm<sup>2</sup>, we observed no change in PFOA concentrations. By using higher electrical current, however, we observed both near linear (zero) and first-order PFAS degradation rates (Figure 2). Based on previous research [25], we believe these observations can be explained by creating kinetic conditions that are either “current-controlled” or “mass-transport controlled”. Under current-controlled conditions, the rate-limiting condition is electron transfer at the BDD anode to form the perfluoroalkyl radical (Figure 1). When PFAS is in abundance (i.e., not limiting), the rate of degradation is constant and controlled by the electron transfer at the BDD interface (i.e., zero-order, Figure 2). Under



mass-transport controlled, the PFAS becomes limiting, and the degradation rate is controlled by the transfer of the PFAS to the BDD electrode (Figure 2). In other words, the reaction becomes concentration-dependent or first-order. By increasing the amperage from 0.2 to 0.4 and 1.0 A, the reaction rate changed from current-controlled to concentration-dependent (Figure 2).

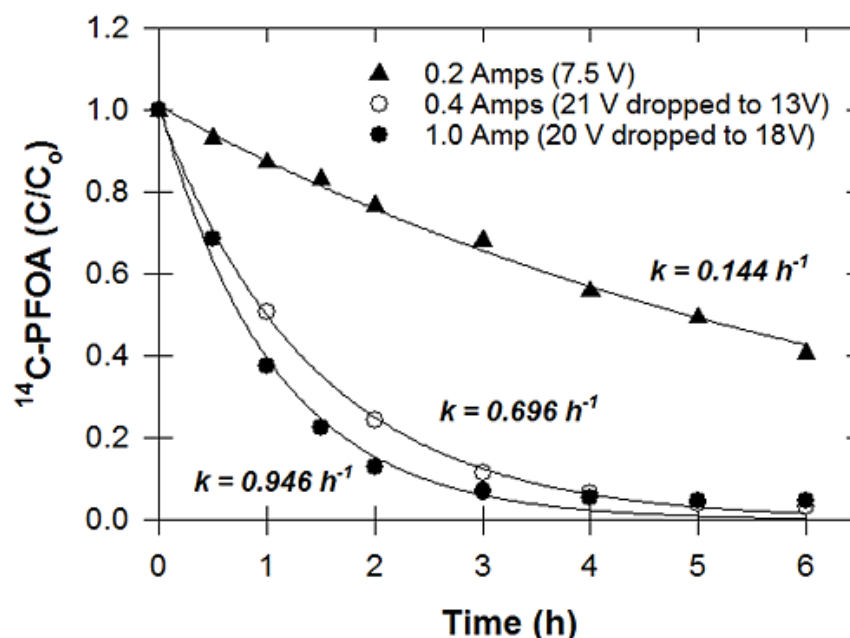


**Figure 2.** Temporal changes in PFOA concentrations under varying electrical currents (0.2, 0.4, and 1.0 A) and current density (8, 16, 40 mA cm<sup>-2</sup>).

### 3.3. pH Adjustment

Previous studies have reported mixed results regarding pH effects on PFAS degradation during electrochemical oxidation [16]. Niu et al. [25] reported that pH affects •OH generation, oxygen overpotential and life span of BDD anodes. Further, lower pH can inhibit oxygen evolution, which can improve PFAS degradation. In most cases, however, pH effects have been reported to be slight to modest. Reasons for the lack of strong pH effects may be attributed, in part, to the lack of true pH-stat conditions. This is due to the surface acidity of the anode, which decreases the solution pH over time. While treating PFOA, Lin et al. [26] recorded bulk pH decreases of 0.5 to 1.5 units during 90 min of electrolysis.

Zhuo et al. [15] tested PFOA degradation by BDD anodes at different pH values (3, 9, 12). They found degradation rates were slightly higher at pH 3 versus 12. Lin et al. [26] similarly treated PFOA by electrochemical oxidation at pH 3, 5, 7, 9, and 11 and found pH 5 produced the highest degradation rate. Nienhauser et al. [27] treated a 4-carbon perfluorobutanesulfonic acid (PFBS), a 6-carbon perfluorohexanesulfonic acid (PFHxS) and an 8-carbon PFOA with EC-BDD at pH 3, 7 and 12; they found little pH effect for PFOA but slower kinetics at pH 12 for the 4- and 6-carbon PFAS. Given these results, we adjusted pH to determine if reaction rates could be increased. Our results of lowering pH provided mixed results in influencing degradation kinetics.

Using two BDD electrodes, the difference between a neutral pH and acidic (pH = 2.5) was negligible (Figure 3A). Moreover, using BDD/Pt/Ti electrodes, we compared degradation rates with and without pH adjustment. Results from two freshly made PFOA solutions showed that pH adjustment did not affect degradation kinetics (Figure 3B). Although pH did not influence degradation, it is noteworthy that the BDD/Pt/Ti electrodes (Figure 3B) produced the fastest degradation kinetics with a first-order rate of 1.478 h<sup>-1</sup> and was greater than the degradation kinetics observed with two BDD (Figure 3A). While this combination was effective, the lifespan of the BDD anode was shortened due to mineral deposits.

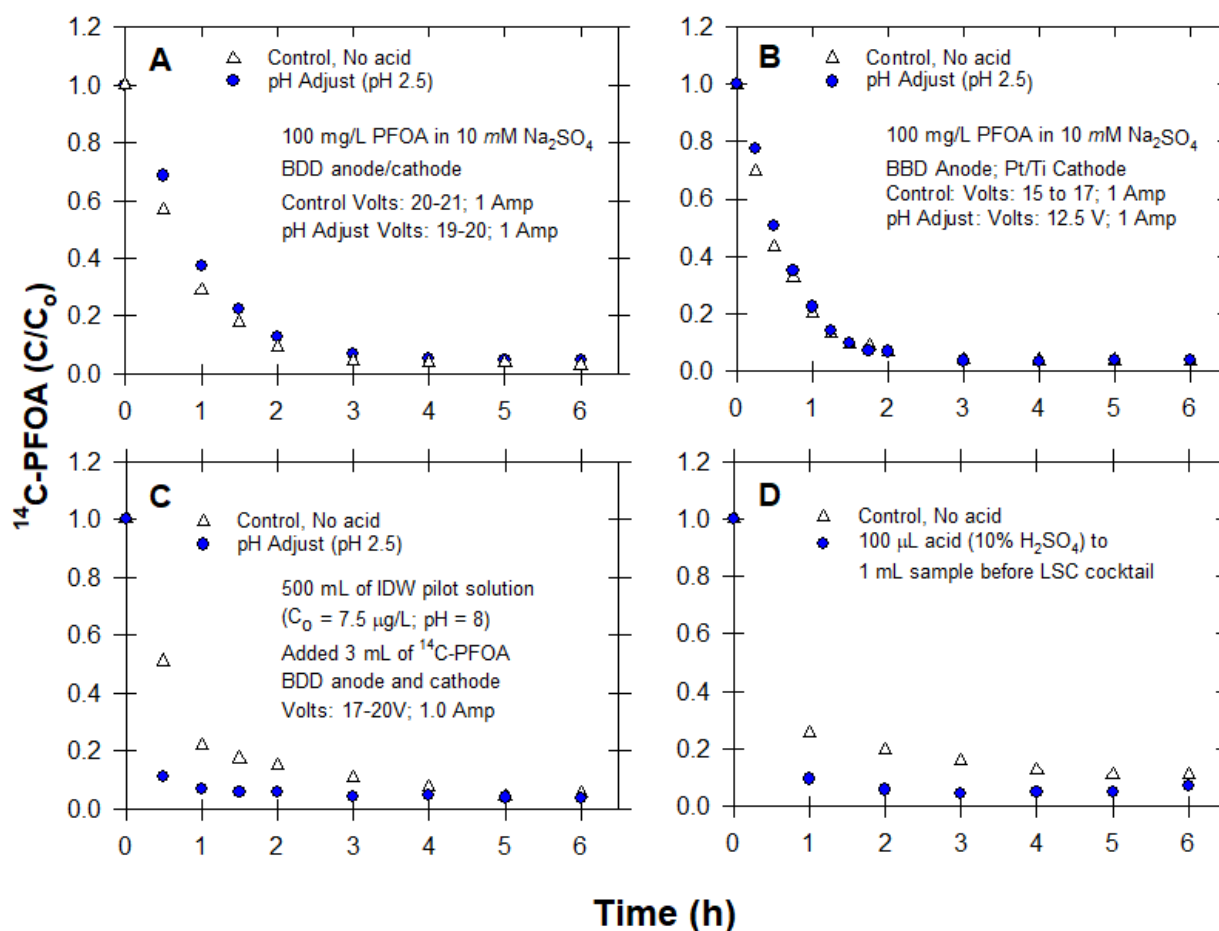


**Figure 3.** (A) Effect of pH adjustment on PFOA kinetics; (B) degradation of  $^{14}\text{C}$ -PFOA with BDD anode and Pt/Ti cathode, with and without pH adjustment; (C) degradation of  $^{14}\text{C}$ -PFOA in alkaline PFOA solution (pH 8) with BDD anode and cathode, with and without pH adjustment (pH adjust = 2.5); (D) effects of acidifying samples before mixing with liquid scintillation counting (LSC) cocktail.

An example where pH appeared to influence degradation rates was when we treated a solution from our pilot-scale IDW barrel (i.e., pilot-scale) with both BDD anodes and cathodes, we observed faster kinetics by lowering the pH (Figure 3C). Given that the IDW barrel solution was alkaline (pH ~8), and not neutral as observed in the previous acidifying experiments (i.e., experiments Figure 3A,B), we determined if the pH effect on PFOA degradation kinetics was real, as reported by Zhuo et al. [15], or an artifact of using temporal changes in  $^{14}\text{C}$ -activity as an indicator of degradation. In other words, electrochemical oxidation of  $^{14}\text{C}$ -PFOA produces  $^{14}\text{CO}_2$  through direct anodic oxidation (Figure 1A) but the produced  $\text{CO}_2$  is more soluble in an alkaline solution than a neutral or acid solution and thus a higher pH may cause some  $^{14}\text{CO}_2$  to stay in solution rather than escape as a gas. If some  $^{14}\text{CO}_2$  stays in solution, then monitoring temporal changes in  $^{14}\text{C}$ -activity includes both  $^{14}\text{C}$  species ( $^{14}\text{C}$ -PFOA +  $^{14}\text{CO}_2$ ) and would yield a degradation rate that is slower than the actual degradation rate. By comparing  $^{14}\text{C}$ -activity of samples acidified versus not acidified before mixing with scintillation cocktail, we showed that an alkaline solution indeed retained some  $^{14}\text{CO}_2$ , if not first acidified (Figure 3D). Thus, when the pH of the  $^{14}\text{C}$ -PFOA solution being treated is not lowered prior to EC treatment, individual samples need to be acidified to drive out any dissolved  $^{14}\text{CO}_2$  in solution.

### 3.4. Electrolyte

Supporting electrolytes are used to provide an electro-conductive medium and minimize the voltage drop and resistance of the electrochemical reactor [15,26]. High electrical conductivity leads to faster electron transport and a better degradation rate for organic pollutants. Zhuo et al. [28] found that the electrochemical oxidation of 6:2 FTS decreased in the trend of  $\text{NaClO}_4 > \text{NaCl} > \text{Na}_2\text{SO}_4$ . To avoid the potential for organochloride byproducts, chlorate, or perchlorate from forming, we compared  $\text{Na}_2\text{SO}_4$  versus  $\text{KH}_2\text{PO}_4$  and found no differences in rate constants (Figure 4). It is important to note that by increasing the salt concentration, lower voltages produced similar amperage. Thus, if amperage or current density was similar ( $8 \text{ mA cm}^{-2}$ , Figure 4), kinetic rates were similar.

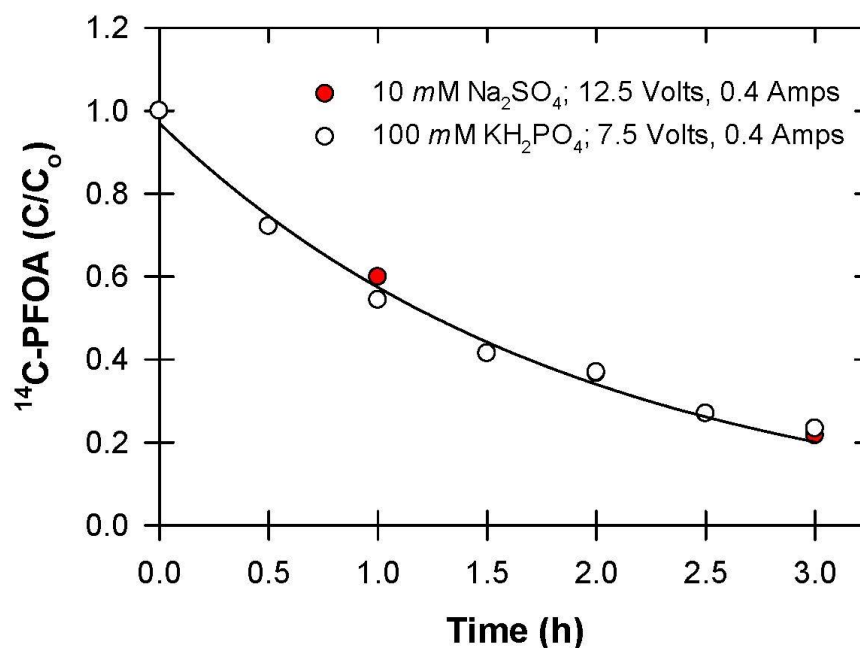


**Figure 4.** Effect of ionic salt and concentration on PFOA degradation by BDD treatment.

### 3.5. Reseeding PFAS to BDD Electrodes

To gain insight into the robustness of the EC-BDD system to continually degrade PFAS, we reseeded PFOA back into the batch reactor. By monitoring disintegrations per minute (dpms) following reseeded of  $^{14}\text{C}$ -PFOA into the BDD-treated solution, the initial drop in dpms increased after the second and third reseedings ( $52\% \rightarrow 65\% \rightarrow 72\%$ , Figure 5A). We also noticed a similar behavior when we electrochemically treated a  $40 \text{ mg L}^{-1}$  fluoride solution before adding  $^{14}\text{C}$ -PFOA (Figure 5B). Results showed that the addition of fluoride increased the initial decrease in  $^{14}\text{C}$ -PFOA (Figure 5B) but caused a plateau; similarly, in a similar but separate experiment using a higher PFOA concentration, the defluorination rate was higher during the first 2 h with BDD electrodes that had been previously exposed to fluoride; but with time, defluorination plateaued after 4 h (Figure 5C). These observations indicate that at least initially, preconditioning the electrodes with fluoride may have altered the electrode surface.

Previous researchers have documented that adsorption of fluoride to the BDD electrodes can occur. Guan et al. [29] observed in their electrochemical system that PFOA decomposed on the BDD anode to generate radicals containing fluorine, which reacted and bonded with the BDD surface. They confirmed this surface adsorption with XPS measurements. Guan et al. [29] also showed that the fluorinated surface showed water repulsion (i.e., more hydrophobic) and suggested that enrichment of the BDD with fluoride may be altering PFAS reaction rates over time. While the fluoride pretreatment may have initially increased defluorination (Figure 5C), it did not last, as observed by the plateau (Figure 5C) and may have promoted additional anodic wear. Anodic wear of BDD can lead

to the formation of oxygenated sites and observable wear of BDD electrodes [30–33]. This changing surface chemistry can affect the reproducibility of electrode performance in water treatment [32].

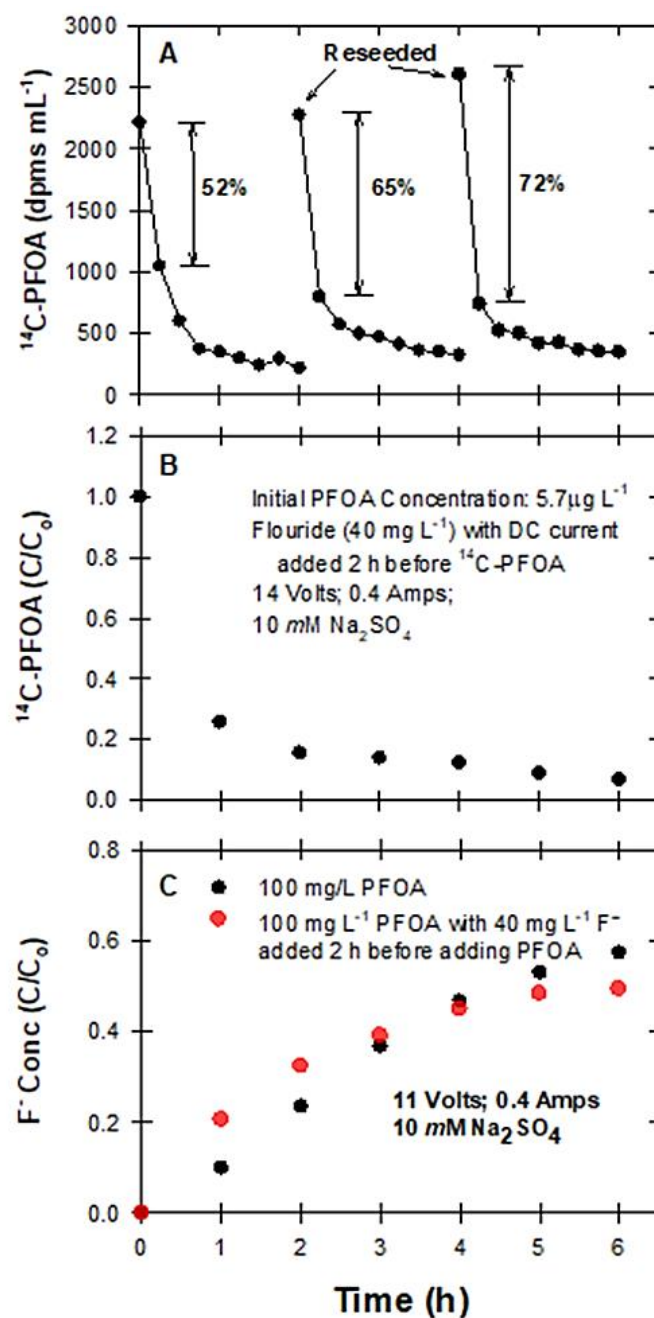


**Figure 5.** (A) Temporal changes in  $^{14}\text{C}$ -PFOA following reseeded; (B) effect of adding fluoride ( $40 \text{ mg L}^{-1}$ ) and treating with BDD electrodes for 2h before adding  $^{14}\text{C}$ -PFOA; (C) fluoride generation from PFOA, with and without preconditioning of BDD electrodes with fluoride ( $40 \text{ mg L}^{-1}$ ).

### 3.6. Defluorination and Fluoride Mass Balance

By using  $^{14}\text{C}$ -labeled PFOA and measuring temporal loss of  $^{14}\text{C}$ -activity and fluoride generation, we were able to quantify the transformation rate of the parent structure (i.e.,  $^{14}\text{C}$ -PFOA) as well as the transformation of the subsequently formed shorter chain degradation products (Figure 6). Results showed nearly complete transformation of the PFOA molecule with approximately 60% defluorination (Figure 6). Both PFOA removal

and  $F^-$  generation plateaued after approximately 3 h with defluorination occurring at a slightly lower rate than PFOA degradation (Figure 6).

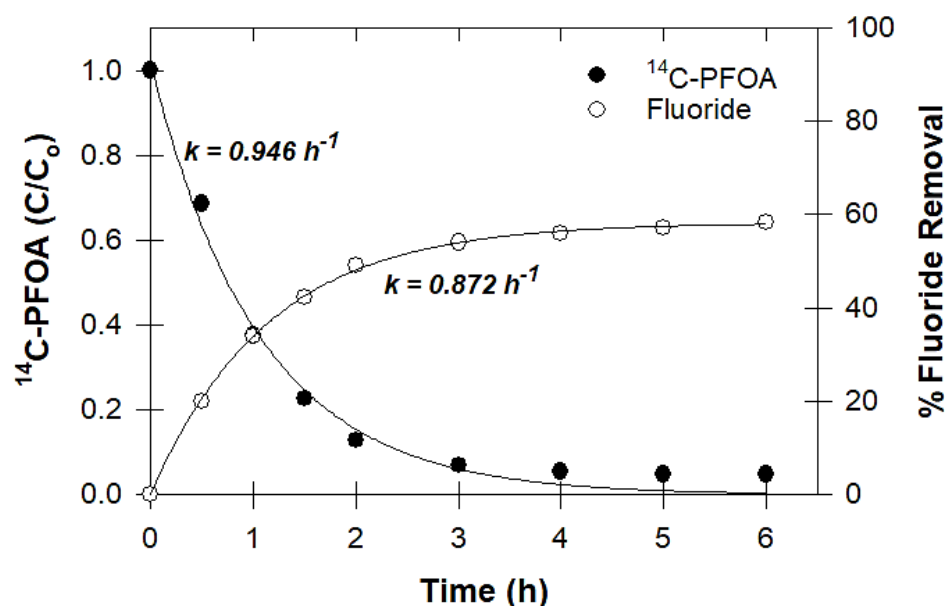


**Figure 6.** Temporal changes in  $^{14}C\text{-PFOA}$  and fluoride concentrations. Experimental conditions: BDD anode and cathode;  $100\text{ mg L}^{-1}$  PFOA, acidified, 20 V, 1 A.

Uwayezu et al. [34] used similar direct current EC-BDD conditions in treating PFOA, and reported 99.5% PFOA degradation and 50% fluoride recovery. They also confirmed the detection of shorter chain (4, 5, 6, and 7 carbon) fluorinated carboxylates. Zhou et al. [15] similarly documented the formation of shorter chain perfluorinated carboxylates following BDD treatment of both PFOA and PFOS. Given that shorter chain perfluorinated compounds are being formed by the EC-BDD treatment (Figure 1) and we observed defluorination rates slowed down after 3 h of treatment (Figure 6), we investigated defluorination rates of various chain length perfluorinated carbonates by using them as starting substrates (Table 1). In these experiments, we used the same starting molar concentration ( $0.24\text{ mM}$ ). Our goal was to determine if any of the shorter chain perfluorinated compounds were resistant to electrochemical oxidation via the EC-BDD treatment. These results confirmed that the shorter chain degradation products formed during the destruction of the parent PFOA or PFOS (Figure 1) were also mineralized by the EC-BDD treatment method.

Results showed that fluoride generated from the perfluorinated compounds were generally linear during the first 3 to 5 h (Figure 7A) with the longer chain length compounds producing a higher percentage of defluorination. Although defluorination rates were slightly slower for the shorter chain compounds, our results confirm that these compounds were not resistant to EC-BDD oxidation. Radjenovic et al. [16] reported that longer chain PFAS are more hydrophobic and have a higher affinity to adsorb to electrode surfaces than shorter chain PFAS, and that this would enhance electrooxidation and defluorination. Barisci and Suri [35] specifically treated short and long chain perfluorocarboxylic acids with Si/BDD electrodes and found overall defluorination was greater with longer carbon chain lengths. Short chain PFAS are characterized as having lower molecular polarizabilities [36], which is the ability of a compound to form a dipole in an electrical field, and is the one molecular descriptor that corresponds with observed reaction rates of PFAS treated by electrochemical oxidation [16,36].

Given that we have observed both zero-order and first-order removal rates of PFOA under varying conditions (Figure 2), we determined initial concentration effects on defluorination rates. Results showed that higher fluoride recovery rates were observed at higher concentrations (Figure 7B), but all concentrations plateaued after approximately 3 h.

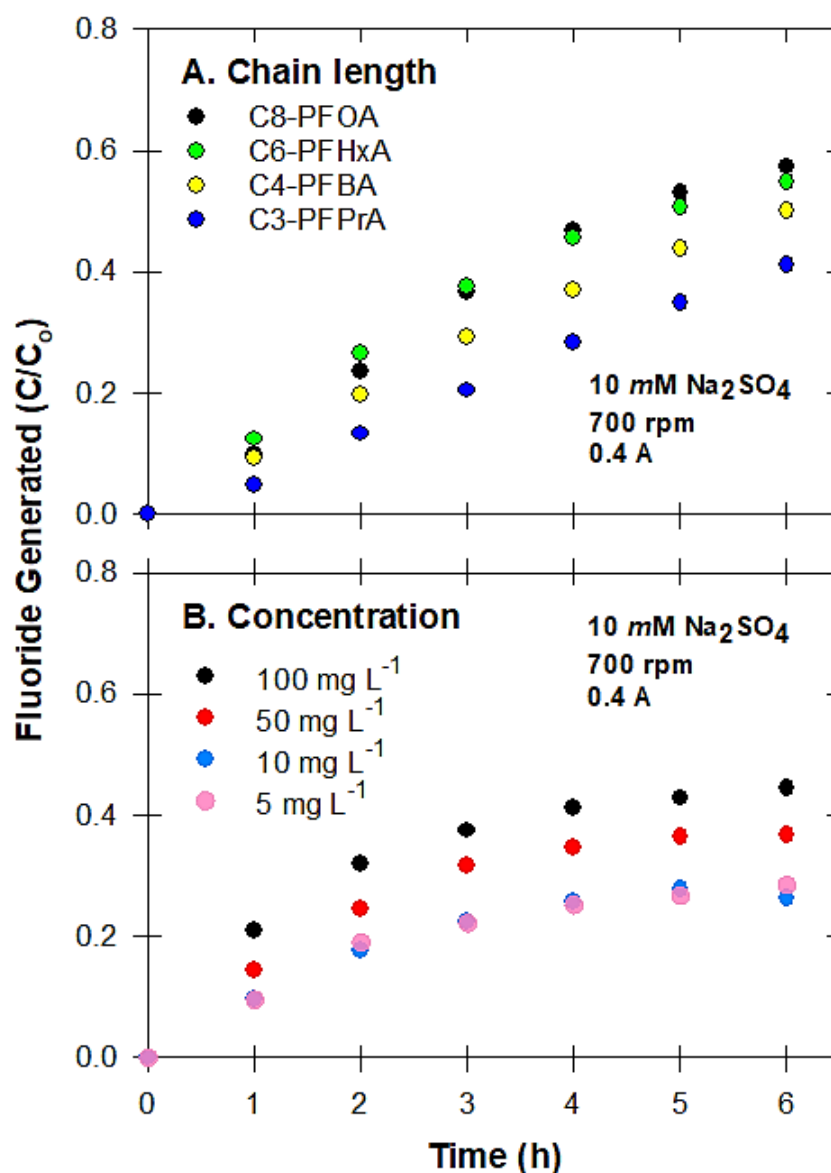


**Figure 7.** (A) Effects of initial concentration on defluorination rates; (B) defluorination rates of various carbon chain length perfluorinated carbonates.

### 3.7. Pilot-Scale Experiments

The custom printed 3D reactor was designed to be compatible with 2 or 4 BDD electrodes and suitable for treating a 208-L container (Figure 8). Before pilot-testing of the 3D reactor with 189 L of PFAS water, the 3D reactor was tested by treating <sup>14</sup>C-PFOA in the laboratory (2 L). By using only <sup>14</sup>C-PFOA (no unlabeled PFOA), the initial concentration was in the 8 to 10 µg L<sup>-1</sup> (ppb) range, which was calculated from the specific activity (µCi mmol<sup>-1</sup>) of the PFOA.

Laboratory results using <sup>14</sup>C-PFOA and the 3D reactor with different power sources (pilot-scale vs. laboratory-scale) showed that reaction rates could be influenced by adjusting the number of electrodes, power sources and polarity (Figure 9). By using 4 BDD electrodes over 2 BDD, reaction rates increased from  $k = 0.738 \text{ h}^{-1}$  to  $1.256 \text{ h}^{-1}$  (Figure 9). Similarly, using two power sources was superior to a single power source ( $k = 0.855$  vs.  $1.577 \text{ h}^{-1}$ ) and by switching the polarity of the electrodes every 30 s, degradation rates were greater than rates obtained using a constant polarity ( $k = 0.854$  vs.  $1.256 \text{ h}^{-1}$ ) (Figure 9).

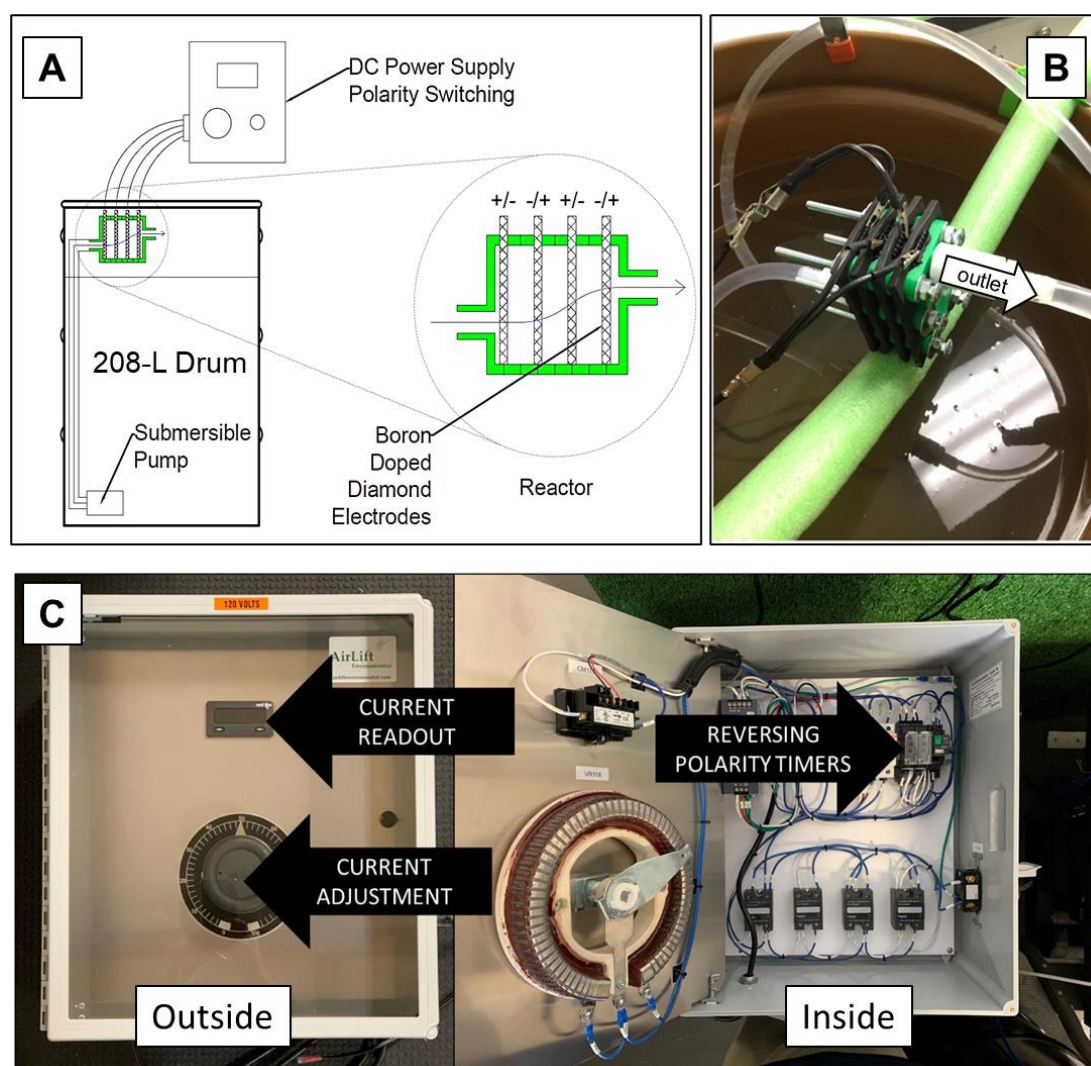


**Figure 8.** (A) Schematic of 208 L barrel experiment with components consisting of barrel, direct-current power supply, and 3D printed, four-BDD electrode chamber; (B) photograph of 3D printed electrode chamber; (C) photograph of direct current power supply.

Results from our 208 L pilot-scale experiment using LC/MS/MS analysis indicated that micrograms per liter (ppb) PFAS concentrations can easily be degraded by electrochemical oxidation using BDD anodes. The pilot-scale reactor and pump moved liquid at  $2.33 \text{ L min}^{-1}$ , meaning the 189 L of simulated IDW was cycled through the 3D reactor every 81 min. Results showed that PFOS was transformed relatively quickly and was below detection in less than 200 h. By contrast, PFOA was transformed approximately three times slower and was reduced to  $0.114 \mu\text{g L}^{-1}$  at the end of the experiment. In a preliminary batch experiment, we also observed faster kinetics with PFOS over PFOA (Figure S1). Using a BDD flow-through reactor, Maldonado et al. [37] also observed faster kinetics with PFOS than PFOA. Nienhauser et al. [27] also found that 4, 6, and 8-carbon PFASs with a sulfonated head group degraded 2–3 times faster than their carboxylic counterparts. Radjenovic et al. [16] noted however, how reactions rates of mixed PFAS could be influenced by starting concentrations. For instance, Liang et al. [38] showed that at PFOA and PFOS concentrations of  $10 \text{ mg L}^{-1}$ , PFOS degradation was slower in the presence of PFOA, whereas Wang et al. [36] working with microgram per liter concentrations observed similar rate constants of perfluoroalkyl acids when treated individually or in mixtures. Fenti et al. [39], who used a Magnéli-phase  $\text{Ti}_n\text{O}_{2n-1}$  mesh anode in a flow-through electrochemical reactor reported faster kinetics for PFOA ( $0.033 \text{ h}^{-1}$ ) than PFOS ( $0.022 \text{ h}^{-1}$ ); these

rate constants reported by Fenti et al. [39] are in the range similar to those observed in our pilot-scale experiment (Figure 10). Given EPA's new health advisory levels for PFOA and PFOS ( $0.004 \text{ ng L}^{-1}$  for PFOA and  $0.02 \text{ ng L}^{-1}$  for PFOS), additional treatment time would be needed for PFOA destruction under the current treatment.

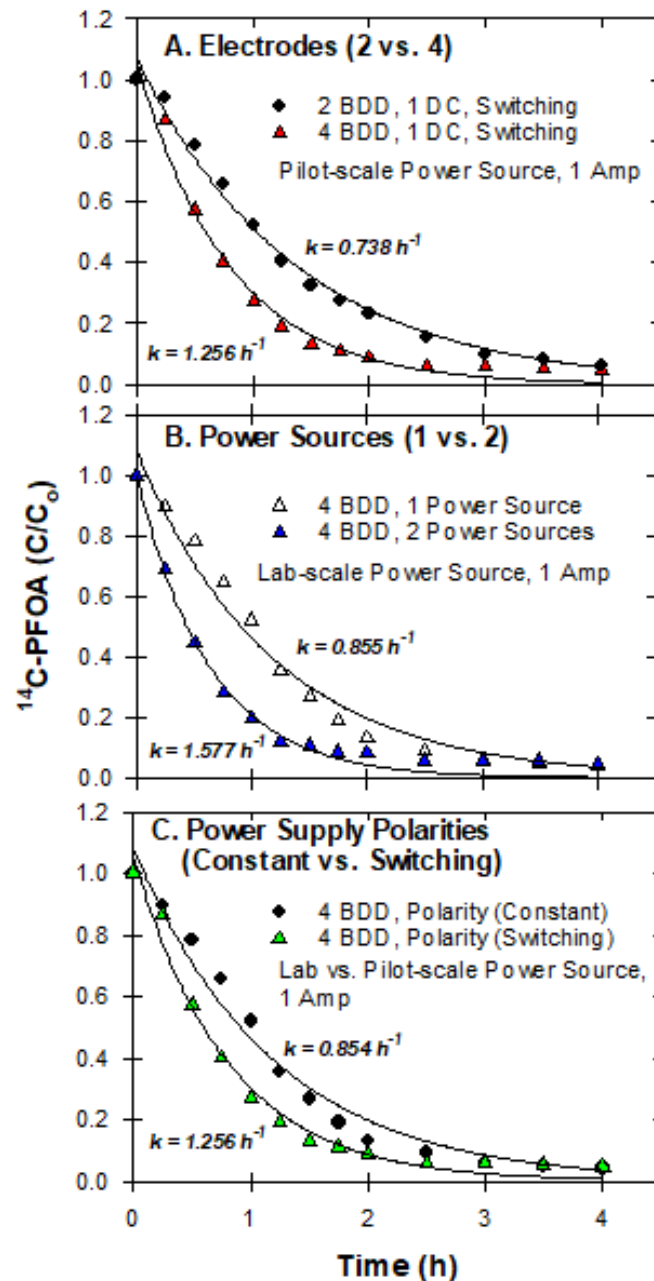


**Figure 9.** Temporal changes in  $^{14}\text{C-PFOA}$  when treated with 3D printed reactor using: (A) 2 versus 4 BDD electrodes; (B) 1 versus 2 power sources; and (C) constant versus switching polarities.

At the end of the pilot-scale experiment, the BDD reactor was disassembled and photographed (Figure 11). Although polarity was switched every thirty seconds, the inflow of the IDW solution through the 3D reactor remained constant and, therefore, all IDW solution entered the same port. This resulted in a buildup of salt on the first BDD electrode (Figure 11). Adding an additional valve to periodically reverse flow direction during the treatment of the IDW may help to alleviate salt buildup in future tests.



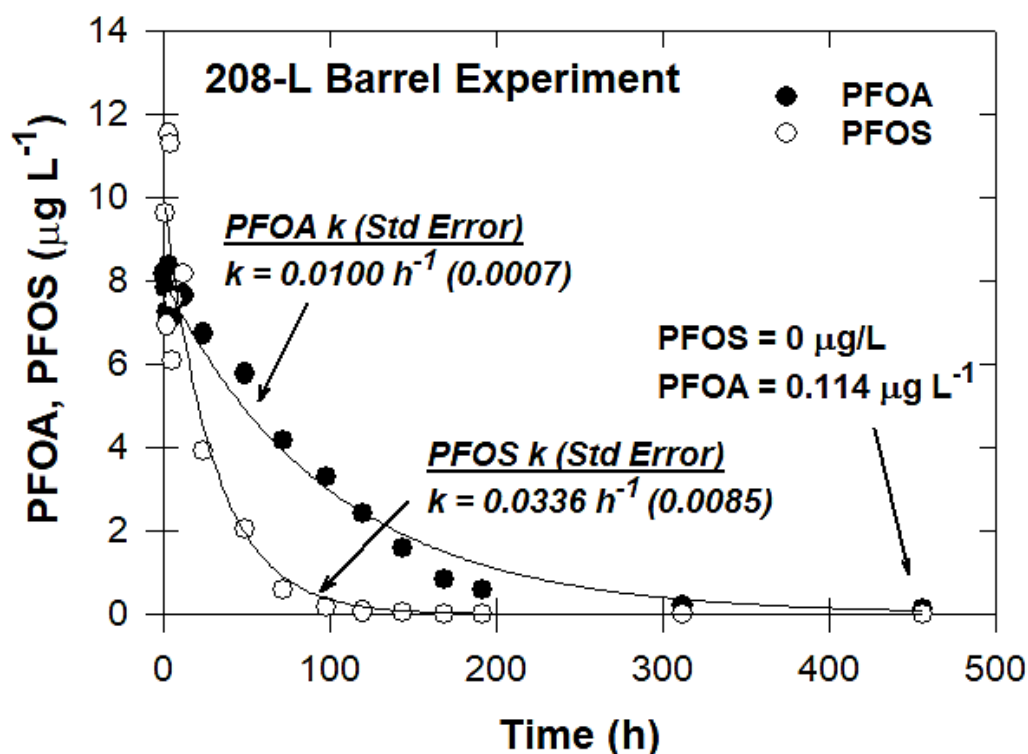


**Figure 10.** Temporal changes in PFOA and PFOS concentrations in 208 L barrel pilot-scale experiment.

Given only synthetic solutions of IDW were tested in this study, we acknowledge treating actual IDW is a logical progression and will be more challenging. Other researchers have been successful in treating real world solutions, such as landfill leachates. Maldonado et al. [36] found that PFOS and PFOA degradation was six times slower in a landfill leachate matrix than in a water matrix using similar conditions (current density, flow through cell); they attributed the slower kinetics to the presence of co-contaminants in the landfill leachate. While treating an ion exchange regenerant, Maldonado et al. [40] found PFAS reaction kinetics were three-fold slower than a synthetic solution and attributed the difference to the presence of co-contaminants.

While the costs of BDD electrodes remain high and a potential roadblock to full scale use, alternative electrodes, such as Magnéli-phase  $\text{Ti}_4\text{O}_7$  anodes offer a lower cost alternative [36]. The use of the electrodes in batch, flow-by and flow-through modes is also a consideration, especially when treating larger quantities of IDW. While more elaborate BDD electrode reactor assemblies have been successfully used in the past [40,41], with some being commercially available (ElectroCell, Amherst, NY, USA), we showed herein, that a low-cost, 3D-printed reactor was functional and capable of treating larger volumes (189 L) of PFAS-contaminated water at a modest cost. Material costs for the printed 3D reactor were less than USD 100. The cost of the additional main components included the four commercial BDD electrodes (USD 1180, NeoCoat<sup>®</sup>, La Chaux-de Fonds, Switzerland), and the custom designed direct current system (USD 2668, 3E, Windsor Heights, IA, USA).

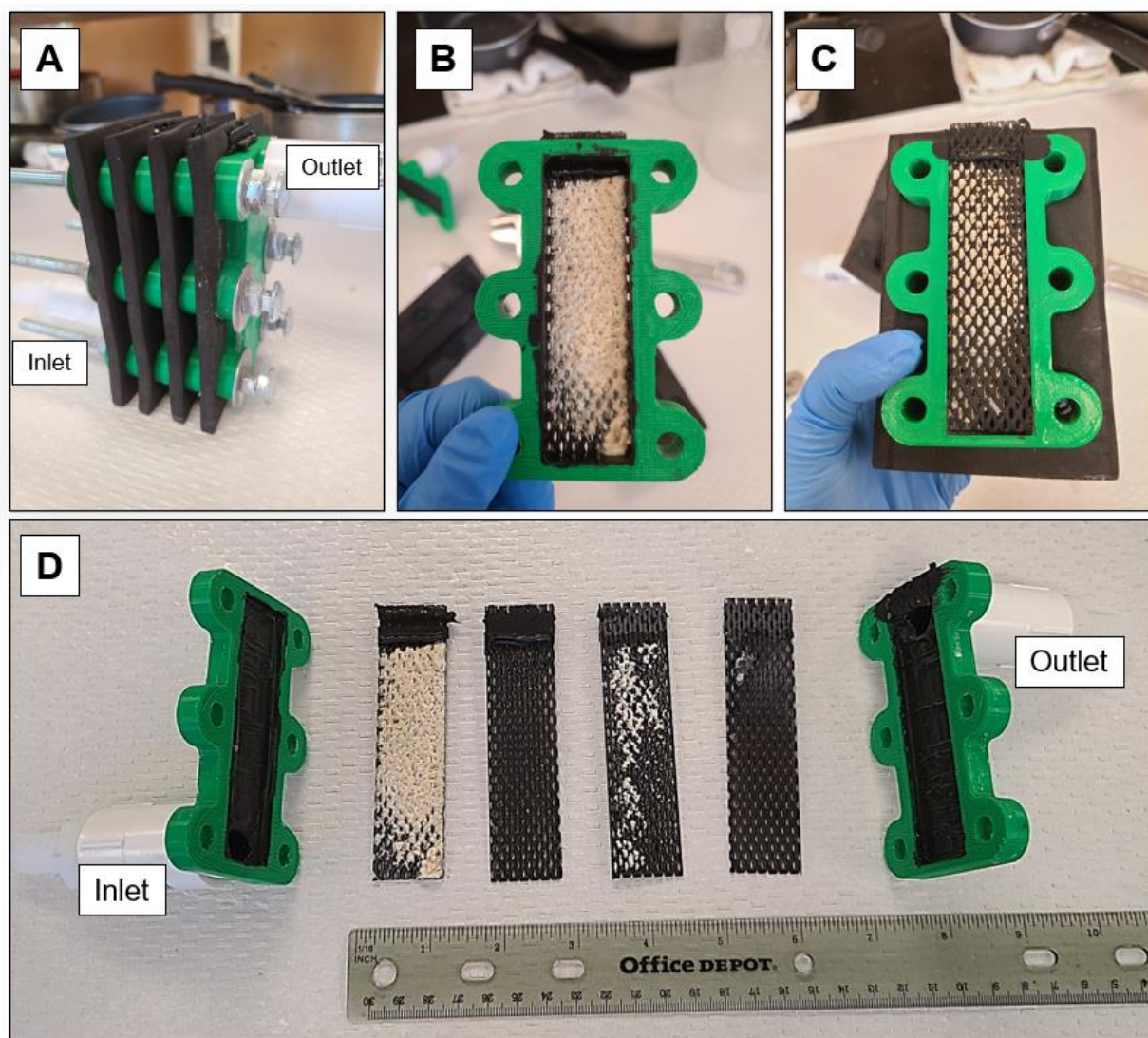


**Figure 11.** Photographs of pilot-scale BDD reactor after treatment: (A) before disassembly. (B) first BDD electrode (front side facing incoming solution) and (C) back side of first electrode. (D) Front side of all 4 BDD electrodes.

#### 4. Conclusions

A series of laboratory and pilot scale experiments were performed to quantify the efficacy of electrochemical oxidation of PFAS using boron-doped diamond electrodes. By using  $^{14}\text{C}$ -labeled PFOA, we showed that low concentrations of PFOA ( $\mu\text{g L}^{-1}$ ) could easily be measured with a liquid scintillation counter and reaction kinetics quantified without the concern of cross contamination. By tracking temporal changes in both  $^{14}\text{C}$ -activity and fluoride concentrations, we showed oxidation of the carboxylic head ( $^{-14}\text{COOH}$  to  $^{14}\text{CO}_2$ ) was possible, and up to 60% of the bonded fluorine was released into the solution. We showed that the shorter chain degradation products formed during the destruction of the parent contaminant were also degraded and defluorinated by the EC-BDD treatment. LC/MS/MS analysis indicated micrograms per liter (ppb) PFAS concentrations were easily degraded by electrochemical oxidation using BDD electrodes. By increasing current density (amperage), observed kinetics changed from current-controlled (zero-order) to mass-transfer controlled (first-order). Reversing polarity improved the lifespan of the BDD electrodes. A low-cost, 3D printed, four-electrode BDD reactor was successful in treating 189 L of simulated IDW in a 208-L container. Periodically alternating the flow direction of the IDW into the 3D reactor may reduce salt buildup and improve performance.

**Supplementary Materials:** The following supporting information can be downloaded at: <https://www.mdpi.com/article/10.3390/w14172708/s1>, Figure S1: Temporal changes in PFOS and PFOA concentrations following treatment with EC-BDD.

**Author Contributions:** Conceptualization, A.Y., E.W., C.E.H., M.C. and S.C.; methodology, A.Y., E.W. and M.C.; validation, A.Y. and E.W.; formal analysis, S.C.; resources, M.C. and S.C.; writing—original draft preparation, A.Y., E.W. and S.C.; writing—review and editing, A.Y., E.W., C.E.H., M.C. and S.C.; funding acquisition, M.C. and S.C. All authors have read and agreed to the published version of the manuscript.

**Funding:** This research was supported by the University of Nebraska–Lincoln School of Natural Resources and Water Science Laboratory with funding from the U.S. Environmental Protection Agency Small Business Innovation Research Program (EPA SBIR, Contract: 68HERC20C0033) and the Nebraska Department of Economic Development’s matching SBIR grant program (Contract: 20-01-074).

**Institutional Review Board Statement:** Not Applicable.

**Informed Consent Statement:** Not Applicable.

**Data Availability Statement:** Not applicable.

**Acknowledgments:** We thank James Reece (AirLift Environmental) for assistance with research and data collection.

**Conflicts of Interest:** The authors declare no conflict of interest.

## References

1. Copp, T. DoD: At least 126 bases report water contaminants linked to cancer, birth defects. *Military Times*, 26 April 2018.
2. Moody, C.A.; Field, J.A. Determination of perfluorocarboxylates in groundwater impacted by fire-fighting activity. *Environ. Sci. Technol.* **1999**, *33*, 2800–2806. [[CrossRef](#)]
3. Moody, C.A.; Hebert, G.N.; Strauss, S.H.; Field, J.A. Occurrence and persistence of perfluorooctanesulfonate and other perfluorinated surfactants in groundwater at a fire-training area at Wurtsmith Air Force Base, Michigan, USA. *J. Environ. Monit.* **2003**, *5*, 341–345. [[CrossRef](#)] [[PubMed](#)]
4. Schultz, M.M.; Barofsky, D.F.; Field, J.A. Quantitative determination of fluorotelomer sulfonates in groundwater by LC MS/MS. *Environ. Sci. Technol.* **2004**, *38*, 1828–1835. [[CrossRef](#)] [[PubMed](#)]
5. Suthersan, S.S.; Horst, J.; Ross, I.; Kalve, E.; Quinnan, J.; Houtz, E.; Burdick, J. Responding to emerging contaminant impacts: Situational management. *Groundw. Monit. Remediat.* **2016**, *36*, 22–32. [[CrossRef](#)]
6. Key, B.L.; Howell, R.D.; Criddle, C.S. Fluorinated organics in the biosphere. *Environ. Sci. Technol.* **1997**, *31*, 2445–2454. [[CrossRef](#)]
7. O’Hagan, D. Understanding organofluorine chemistry. An introduction to the C-F bond. *Chem Soc. Rev.* **2008**, *37*, 308–318. [[CrossRef](#)]
8. Conder, J.M.; Hoke, R.A.; Wolf, W.D.; Russell, M.H.; Buck, R.C. Are PFCA’s Bioaccumulative? A critical review and comparison with regulatory criteria and persistent lipophilic compounds. *Environ. Sci. Technol.* **2008**, *42*, 995–1003. [[CrossRef](#)]
9. Lau, C.; Anitole, K.; Hodes, C.; Lai, D.; Pfahles-Hutchens, A.; Seed, J. Perfluoroalkyl acids: A review of monitoring and toxicological findings. *Toxicol. Sci.* **2007**, *99*, 366–394. [[CrossRef](#)]
10. Johansson, N.; Eriksson, P.; Viberg, H. Neonatal exposure to PFOS and PFOA in mice results in changes in proteins which are important for neuronal growth and synaptogenesis in the developing brain. *Toxicol. Sci.* **2009**, *108*, 412–418. [[CrossRef](#)]
11. Liu, W.; Xu, X.L.; Li, X.; Jin, Y.H.; Sasaki, K.; Saito, N.; Sato, I.; Tsuda, S. Human nails analysis as biomarker of exposure to perfluoroalkyl compounds. *Environ. Sci. Technol.* **2011**, *45*, 8144–8150. [[CrossRef](#)]
12. United States Environmental Protection Agency. EPA Announces New Drinking Water Health Advisories for PFAS Chemicals, \$1 Billion in Bipartisan Infrastructure Law Funding to Strengthen Health Protections | US EPA. 2022. Available online: <https://www.epa.gov/newsreleases/epa-announces-new-drinking-water-health-advisories-pfas-chemicals-1-billion-bipartisan> (accessed on 30 July 2022).
13. Crunden, E.A. Defense department hits the brakes on PFAS incineration. E&E PM News. 2022. Available online: <https://www.eenews.net/articles/defense-department-hits-the-brakes-on-pfas-incineration/> (accessed on 30 July 2022).
14. United States Environmental Protection Agency. PFAS Innovative Treatment Team (PITT). 2020. Available online: <https://www.epa.gov/chemical-research/pfas-innovative-treatment-team-pitt> (accessed on 15 March 2022).
15. Zhuo, Q.; Deng, S.; Yang, B.; Huang, J.; Wang, B.; Zhang, T.; Yu, G. Degradation of perfluorinated compounds on a boron-doped diamond electrode. *Electrochim. Acta* **2012**, *77*, 17–22. [[CrossRef](#)]
16. Radjenovic, J.; Duinslaeger, N.; Avvl, S.S.; Chaplin, B.P. Facing the challenge of poly- and perfluoroalkyl substances in water: Is electrochemical oxidation the answer? *Environ. Sci. Technol.* **2020**, *54*, 14815–14829. [[CrossRef](#)] [[PubMed](#)]

17. United States Environmental Protection Agency. Method 533: Determination of Per- and Polyfluoroalkyl Substances in Drinking Water by Isotope Dilution Anion Exchange Solid Phase Extraction and Liquid Chromatography/Tandem Mass Spectrometry | US EPA. 2019. Available online: <https://www.epa.gov/dwanalyticalmethods/method-533-determination-and-polyfluoroalkyl-substances-drinking-water-isotope> (accessed on 30 July 2022).
18. Carter, K.E.; Farrel, J. Oxidative destruction of perfluorooctane sulfate using boron-doped diamond film electrodes. *Environ. Sci. Technol.* **2009**, *42*, 6111–6115. [[CrossRef](#)] [[PubMed](#)]
19. Liao, Z.; Farrell, J. Electrochemical oxidation of perfluorobutane sulfonate using boron-doped diamond film electrodes. *J. Appl. Electrochem.* **2009**, *39*, 1993–1999. [[CrossRef](#)]
20. Matzek, L.W.; Tipton, M.J.; Farmer, A.T.; Steen, A.D.; Carter, K.E. Understanding electrochemically activated persulfate and its application to Ciprofloxacin abatement. *Environ. Sci. Technol.* **2018**, *52*, 5875–5883. [[CrossRef](#)]
21. Schaefer, C.E.; Andaya, C.; Urteaga, A.; McKenzie, E.R.; Higgins, C.P. Electrochemical treatment of perfluorooctanoic acid (PFOA) and perfluorooctane sulfonic acid (PFOS) in groundwater impacted by aqueous film forming foams (AFFFs). *J. Hazard. Mater.* **2015**, *295*, 170–175. [[CrossRef](#)]
22. Schaefer, C.E.; Andaya, C.; Burant, A.; Condee, C.W.; Urteaga, A.; Strathmann, T.J.; Higgins, C.P. Electrochemical treatment of perfluorooctanoic acid and perfluorooctane sulfonate: Insights into mechanisms and application to groundwater treatment. *Chem. Eng. J.* **2017**, *317*, 424–432. [[CrossRef](#)]
23. Kapalka, A.; Fóti, G.; Comninellis, C. Kinetic modelling of electrochemical mineralization of organic pollutants for wastewater treatment. *J. Appl. Electrochem.* **2008**, *38*, 7–16. [[CrossRef](#)]
24. Ochiai, T.; Iizuka, Y.; Nakata, K.; Murakami, T.; Tryk, D.A.; Fujishima, A.; Koide, Y.; Morito, Y. Efficient electrochemical decomposition of perfluorocarboxylic acids by the use of a boron-doped diamond electrode. *Diam. Relat. Mater.* **2011**, *20*, 64–67. [[CrossRef](#)]
25. Niu, J.; Li, Y.; Shang, E.; Xu, Z.; Liu, J. Electrochemical oxidation of perfluorinated compounds in water. *Chemosphere* **2016**, *146*, 526–538. [[CrossRef](#)]
26. Lin, H.; Niu, J.; Ding, S.; Zhang, L. Electrochemical degradation of per-fluorooctanoic acid (PFOA) by Ti/SnO<sub>2</sub>-Sb, Ti/SnO<sub>2</sub>-Sb/PbO<sub>2</sub> and Ti/SnO<sub>2</sub>-Sb/MnO<sub>2</sub> anodes. *Water Res.* **2012**, *46*, 2281–2289. [[CrossRef](#)] [[PubMed](#)]
27. Nienhauser, A.B.; Ersan, M.S.; Lin, Z.; Perreault, F.; Westerhoff, P. Boron-doped diamond electrodes degrade short- and long-chain per- and polyfluorinated alkyl substances in real industrial wastewaters. *J. Environ. Chem. Eng.* **2022**, *10*, 107192. [[CrossRef](#)]
28. Zhuo, Q.; Li, X.; Yan, F.; Yang, B.; Deng, S.; Huang, J.; Yu, G. Electrochemical oxidation of 1H, 1H, 2H, 2H-perfluorooctane sulfonic acid (6:2 FTS) on DSA electrode: Operating parameters and mechanism. *J. Environ. Sci.* **2014**, *26*, 1733–1739. [[CrossRef](#)] [[PubMed](#)]
29. Guan, B.; Zhi, J.; Zhang, X.; Murakami, T.; Fujishima, A. Electrochemical route for fluorinated modification of boron-doped diamond surface with perfluorooctanoic acid. *Electrochem. Commun.* **2007**, *9*, 2817–2821. [[CrossRef](#)]
30. Carrillo-Abad, J.; Perez-Herranz, V.; Urteaga, A. Electrochemical oxidation of 6:2 fluorotelomer sulfonic acid (6:2 FTSA) on BDD: Electrode characterization and mechanistic investigation. *J. Appl. Electrochem.* **2018**, *48*, 589–596. [[CrossRef](#)]
31. Chaplin, B.P.; Wylie, I.; Zheng, H.; Carlisle, J.A.; Farrell, J. Characterization of the performance and failure mechanisms of boron-doped diamond ultrananocrystalline diamond electrodes. *J. Appl. Electrochem.* **2011**, *41*, 1329–1340. [[CrossRef](#)]
32. Chaplin, B.P.; Hubler, D.K.; Farrell, J. Understanding anodic wear at boron doped diamond film electrodes. *Electrochim. Acta* **2013**, *89*, 122–131. [[CrossRef](#)]
33. Duo, I.; Levy-Clement, C.; Fujishima, A.; Comninellis, C. Electron transfer kinetics on boron-doped diamond Part I: Influence of anodic treatment. *J. Appl. Electrochem.* **2004**, *34*, 935–943. [[CrossRef](#)]
34. Uwayezu, J.N.; Carabante, I.; Lejon, T.; van Hees, P.; Karlsson, P.; Hollman, P.; Kumpiene, J. Electrochemical degradation of per- and poly-fluoroalkyl substances using boron-doped diamond electrodes. *J. Environ. Manag.* **2021**, *290*, 112573. [[CrossRef](#)]
35. Barisci, S.; Suri, R. Electrooxidation of short and long chain perfluorocarboxylic acids using boron doped diamond electrodes. *Chemosphere* **2020**, *243*, 125349. [[CrossRef](#)]
36. Wang, Y.; Pierce, R.D.; Shi, H.; Li, C.; Huang, Q. Electrochemical degradation of perfluoroalkyl acids by titanium suboxides anodes. *Environ. Sci. Water Res. Technol.* **2020**, *6*, 144–152. [[CrossRef](#)]
37. Maldonado, Y.; Landi, G.M.; Ensich, M.; Becker, M.F.; Witt, S.E.; Rusinek, C.A. A flow-through cell for the electrochemical oxidation of perfluoroalkyl substances in landfill leachates. *J. Water Process Eng.* **2021**, *43*, 102210. [[CrossRef](#)]
38. Liang, S.; Pierce, R.D., Jr.; Lin, H.; Chiang, S.-Y.D.; Huang, Q.J. Electrochemical oxidation of PFOA and PFOS in concentrated waste streams. *Remediation* **2018**, *28*, 127–134. [[CrossRef](#)]
39. Fenti, A.; Jin, Y.; Rhoades, A.J.H.; Dooley, G.P.; Iovino, P.; Salvestrini, S.; Musmarra, D.; Mahendra, S.; Peaslee, G.F.; Blotvogel, J. Performance testing of mesh anodes for in situ electrochemical oxidation of PFAS. *Chem. Eng. J. Adv.* **2022**, *9*, 100205. [[CrossRef](#)]
40. Maldonado, Y.; Becker, M.F.; Nickelsen, M.G.; Witt, S.E. Laboratory and semi-pilot scale study on the electrochemical treatment of perfluoroalkyl acids from ion exchange still bottoms. *Water* **2021**, *13*, 2873. [[CrossRef](#)]
41. Witt, S.; Rancis, N.; Ensich, M.; Maldonado, V. Electrochemical destruction of “Forever Chemicals”: The right solution at the right time. *Electrochem. Soc. Interface* **2020**, *29*, 73–76. [[CrossRef](#)]